Processing of thin SU-8 films

2008 J. Micromech. Microeng. 18 125020

(http://iopscience.iop.org/0960-1317/18/12/125020)

J. Micromech. Microeng. **18** (2008) 125020 (10pp) doi:10.1088/0960-1317/18/12/125020

Processing of thin SU-8 films

Stephan Keller[1], **Gabriela Blagoi, Michael Lillemose, Daniel Haefliger and Anja Boisen**

DTU Nanotech, Department of Micro- and Nanotechnology, Technical University of Denmark, Bldg. 345 East, DK-2800 Kgs. Lyngby, Denmark

E-mail: stephan.keller@nanotech.dtu.dk

Received 19 August 2008, in final form 7 October 2008
Published 14 November 2008
Online at stacks.iop.org/JMM/18/125020

Abstract

This paper summarizes the results of the process optimization for SU-8 films with thicknesses $\leqslant 5\ \mu$m. The influence of soft-bake conditions, exposure dose and post-exposure-bake parameters on residual film stress, structural stability and lithographic resolution was investigated. Conventionally, the SU-8 is soft-baked after spin coating to remove the solvent. After the exposure, a post-exposure bake at a high temperature $T_{\mathrm{PEB}} \geqslant 90\ ^{\circ}$C is required to cross-link the resist. However, for thin SU-8 films this often results in cracking or delamination due to residual film stress. The approach of the process optimization is to keep a considerable amount of the solvent in the SU-8 before exposure to facilitate photo-acid diffusion and to increase the mobility of the monomers. The experiments demonstrate that a replacement of the soft-bake by a short solvent evaporation time at ambient temperature allows cross-linking of the thin SU-8 films even at a low $T_{\mathrm{PEB}} = 50\ ^{\circ}$C. Fourier-transform infrared spectroscopy is used to confirm the increased cross-linking density. The low thermal stress due to the reduced T_{PEB} and the improved structural stability result in crack-free structures and solve the issue of delamination. The knowledge of the influence of different processing parameters on the responses allows the design of optimized processes for thin SU-8 films depending on the specific application.

1. Introduction

The negative epoxy-based photoresist SU-8 was introduced in the early nineties as a thick-film resist suitable for the fabrication of structures with thicknesses of several hundreds of micrometers [1–4]. Initially, the SU-8 was developed as a thick-film resist for the patterning of molds for electroplating in the LIGA process, but very soon it became a popular material in other areas of microfabrication such as microfluidics [5, 6] and optics [7, 8]. The main advantage of the resist is the low absorption coefficient at wavelengths above 300 nm, which allows for the patterning of films with thicknesses in the millimeter range at aspect ratios of up to 20 in a single step of photolithography [9]. High chemical resistance, biocompatibility and structural stability are other factors that have made the SU-8 a widely employed polymer in microfabrication.

SU-8 resist is a chemically amplified photoresist and the main components are SU-8 monomers, organic solvent and a photo-acid generator (PAG). The available film thicknesses depend on the amount of solvent in the resist before spin coating. Conventionally, the deposition of the resist is followed by a soft-bake to remove the solvent. Then, the film is exposed to UV light and patterning is achieved by the use of a photolithographic mask. During this step, the triarylsulfonium hexafluoroantimonate salt serving as the PAG is decomposed and a strong acid is generated [10]. The photo-acid diffuses to the SU-8 monomers and initiates cationic polymerization by opening of the epoxy rings. The formation of a cross-link takes place if another epoxy group is available due to diffusion and rearrangement of the monomers or polymer clusters. The actual mechanism of polymerization using an onium salt as the photo-initiator is quite complex. Different authors tried to model the cross-linking of negative chemically amplified photoresists [11, 12]. Patsis and co-workers conclude on diffusion-controlled polymerization in their study on the Epoxy Cresol Novolak resist (ECR) [13]. This resist has the same photo-initiator as the SU-8, and structure and reaction mechanisms are comparable. Therefore, it is assumed that photo-acid diffusion is the rate-determining step for the polymerization of the SU-8. Compared to this, the relatively

[1] Author to whom correspondence should be addressed.

fast opening of the epoxy rings and the covalent binding between them lead to fast solidification of the monomer network. The high functionality of the SU-8 with an average of eight epoxy groups per monomer further promotes the formation of covalent bonds. In general, the polymerization is accelerated by a post-exposure bake (PEB) at 80–100 °C immediately after exposure. The elevated temperature promotes diffusion of the photo-acid and increases the mobility of the SU-8 monomers, which allows for improved cross-linking. The fast polymerization during the PEB limits photo-acid diffusion into non-exposed areas because of entrapment of the catalytic protons. This so-called cage effect ensures the high resolution of the SU-8 structures [13]. At the same time, polymerization slows down during the PEB due to a decrease in the concentration of the unreacted epoxy groups and decreased mobility of the monomers as a consequence of the increasing cage effect. Finally, the non-cross-linked resist is removed by development in an organic solvent.

As a result of the high interest in the SU-8 for microfabrication, a large amount of work on process optimization has been published. The reports include optimization of soft-bake [14], exposure dose [15, 16] and post-exposure bake [9] not only for UV lithography but also for x-ray and e-beam lithography [17, 18]. Typically, these process optimizations have been carried out for resist films with thicknesses of more than 50 μm and up to several hundreds of micrometers. The main issues have been structural stability, lithographic resolution, straight sidewall profiles and residual stress in the SU-8.

The residual stress in the SU-8 film after processing on a silicon substrate is a combination of intrinsic and extrinsic stress. Intrinsic stress is mostly generated during cross-linking due to the confinement of the monomers in the rigid polymer matrix. Particularly during the first minutes of the PEB, the cross-linking of epoxy resist leads to densification. Further, there is a loss of mass due to solvent evaporation [19]. The shrinkage due to polymerization and solvent evaporation results in tensile intrinsic stress. Extrinsic stress involves an externally applied force or a change in ambient conditions. There, thermal stress is the important component in the case of SU-8 processing. It arises during the temperature cycling involved and is a result of the mismatch of the coefficients of thermal expansion (CTE) of the silicon substrate and SU-8. The thermal stress σ_{th} can be estimated by the following equation [20]:

$$\sigma_{\mathrm{th}} = (\alpha_{\mathrm{SU8}} - \alpha_{\mathrm{Si}}) \frac{E_{\mathrm{SU8}}}{1 - \upsilon_{\mathrm{SU8}}} (T_{\mathrm{PEB}} - T_o). \quad (1)$$

Here, α_{Si} and α_{SU8} are the CTE of the two materials, E_{SU8} and υ_{SU8} are Young's modulus and Poisson's ratio of the SU-8, respectively, T_{PEB} is the PEB temperature and T_o is the ambient temperature. The thermal stress is tensile because the polymer layer contracts more than the silicon substrate during cool-down after the PEB. In a first approximation, thermal stress is not considered before the onset of polymerization of the SU-8 because the Young's modulus for the non-cross-linked SU-8 is assumed to be very low.

In the past few years, a growing number of research groups discovered the SU-8 as a thin-film photoresist. SU-8 films with thickness in the micrometer range can be used as a cladding layer in micro-optics, as a dielectric material for microelectronic circuits or as an etch mask in microfabrication. Freestanding mechanical structures such as cantilevers or membranes with thickness below 10 μm have been fabricated [21–23]. Lithographic resolution is improved as the film thickness is reduced. On the other hand, the structural stability of thin SU-8 films is critical and the in-plane stress results in cracking or delamination from the substrate.

Compared to thick-film processing, the number of publications on processing of thin SU-8 films is very limited. Conventionally, processes optimized for thicker films have simply been adapted. There, the same process temperatures were used but the bake times were shortened and the UV exposure dose was reduced [24]. This report presents to our knowledge the first detailed experimental study on processing of thin SU-8 films with thicknesses $t \leqslant 5$ μm. Two approaches were investigated to solve the presented issues.

(i) An increase of the cross-linking density improves the structural stability of the SU-8 and should reduce cracking.
(ii) The in-plane stress generated during processing has to be minimized. For the extrinsic stress described by (1), this can be achieved by lowering the PEB temperature.

As presented above, conventional processing is based on an increase of temperature to facilitate the photo-acid diffusion after UV exposure. The approach of the process optimization is to keep a considerable amount of the solvent in the SU-8 before exposure. This will allow for high mobility of photo-acid and SU-8 monomers and therefore polymerization at a low temperature [14]. The expected result is less thermal stress but sufficient cross-linking to ensure structural stability of the polymer. The investigated responses are film stress, photolithographic resolution, stability toward development and cross-linking density.

2. Materials and method

Standard silicon wafers without previous cleaning or surface treatment were used as a substrate. Approximately 3 ml of SU-8 2002 (MicroChem, USA) was manually dispensed onto the substrate. The spin coating was done on a standard spin coater (RC8, Karl-Süss, France) at 1500 rpm during 30 s with an acceleration of 5000 rpm s^{-1} to achieve a nominal thickness of 2 μm. A programmable hotplate (Harry Gestigkeit GmbH, Germany) that allowed parallel processing of two samples was used for all the baking steps. The ramping rate to the final bake temperatures was constant at 2 °C min^{-1} and the wafers were left on the hotplate for 2 h after the end of the actual bake to allow slow cool-down to ambient temperature. The exposure was done on an UV aligner (MA6/BA6, Karl-Süss, Germany) using a mercury lamp at an intensity of 9 mW cm^{-2}. The aligner was equipped with an i-line filter (365 nm, 20 nm FWHM) because the increased absorption of the SU-8 at shorter wavelengths would jeopardize the resolution. The samples were immersed for 4 min in propylene glycol methyl ether acetate (PGMEA) to remove the non-cross-linked resist. Finally, the SU-8 was rinsed with isopropyl alcohol (IPA) for 30 s and dried in air.

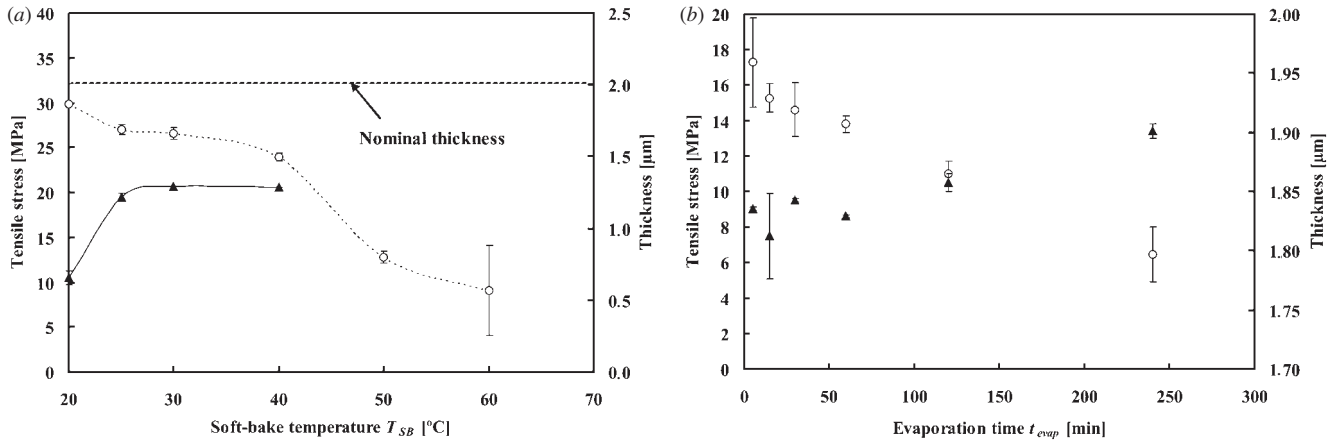

Figure 1. Influence of (*a*) soft-bake temperature T_{SB} ($t_{SB} = 10$ min) and (*b*) evaporation time t_{evap} on thickness (○) and stress (▲) for 2 μm thick SU-8; $D = 200$ mJ cm^{-2}; $T_{PEB} = 40$ °C; $t_{PEB} = 60$ min.

In several series of experiments the parameters of soft-bake, exposure and post-exposure bake (PEB) were varied. For each set of parameters, two samples were processed in parallel resulting in a total number of about 140 wafers for this process optimization. The first sample was patterned by exposure in hard contact mode through a mask. The mask design included test structures of various dimensions to allow the monitoring of the lithographic resolution of the corresponding process. Imaging of lines and trenches with a scanning electron microscope (SEM, FEI Nova 600) followed by image treatment (ImageTool, University of Texas Health Science Center, TX) was used for this purpose. The imaging was performed in low-vacuum mode where a pressure of 0.6 mbar was used to minimize charging of the non-conducting polymer samples. The second sample was flood-exposed and used for the measurement of thickness and film stress. The thickness of the SU-8 was measured with a spectrophotometer (FilmTek, SCI, CA) that allowed automatic mapping on wafer scale samples. For the evaluation of the in-plane stress, the radius of curvature of the silicon substrate before and after processing of the SU-8 was measured with a profilometer (Dektak8, Veeco, Germany). The measured values of the radius of curvature and film thickness allowed the calculation of the residual film stress by Stoney's formula [25]. For each sample, three stress measurements were performed.

In the first part of the optimization, the influence of the solvent content on the processing of the thin SU-8 films was investigated. For this purpose, the soft-bake parameters were varied. Exposure dose $D = 200$ mJ cm^{-2}, PEB temperature $T_{PEB} = 40$ °C and PEB time $t_{PEB} = 60$ min were constant for all the experiments. The selection of a low T_{PEB} should allow for low thermal stress according to (1). In a first experimental series of the soft-bake optimization, the soft-bake temperature T_{SB} was varied between 20 and 60 °C. The soft-bake time t_{SB} was kept constant at 10 min. In a second series of experiments, the soft-bake was completely replaced by a solvent evaporation at ambient temperature ($T_{SB} = 20$ °C). For these samples, an evaporation time t_{evap} was defined as the waiting time between spin coating and exposure of the SU-8 films. This parameter was varied from 5 min to 4 h.

In the second part of the process optimization, exposure dose D, PEB temperature T_{PEB} and PEB time t_{PEB} were the explored variables. An evaporation time $t_{evap} = 30$ min was introduced for all the experiments. For the design of experiments (DoE) of an initial series of screening experiments, the software MODDE 6.0 (Umetrics, Sweden) was used. There, a central composite face (CCF) design consisting of 17 experiments was selected, three of them being the center points used for the evaluation of the reproducibility. This design allows response surface modeling with both second order and interaction terms. The modeling was carried out using MODDE. The models were simplified through removal of insignificant terms and the exclusion of experimental results that were improbable based on statistical testing. The experimental range was $D = 150$–250 mJ cm^{-2}, $T_{PEB} = 30$–50 °C and $t_{PEB} = 30$–120 min. The initial screening experiments allowed the identification of the most important parameters influencing the processing of thin SU-8 films at the selected residual solvent content. Additional experiments were performed extending the parameter range to 100 °C for T_{PEB} and to 500 mJ cm^{-2} for D.

For comparison, samples were fabricated with conventional SU-8 processing. The process, further defined as *Process A*, was similar to the one recommended by the producer and is representative for the schemes that are most commonly used in microfabrication [24]. A two-step soft-bake of 10 min at 60 °C and 10 min at 90 °C with a constant ramping of 10 °C min^{-1} was performed to remove the solvent. The exposure dose was 250–500 mJ cm^{-2}. The PEB was done with the identical parameters as the soft-bake.

3. Influence of solvent content

Figure 1(*a*) shows the measured thickness and the tensile film stress for samples processed at different T_{SB}. Figure 1(*b*) represents the same parameters as a function of t_{evap}. The measurements show that the thickness of the SU-8 films decreases with an increase of T_{SB} and t_{evap}. On the other hand, the tensile film stress decreases with a decrease of T_{SB} and t_{evap}. Stress measurements on samples soft-baked at $T_{SB} >$

40 °C were impossible due to the non-uniformity of the SU-8 films.

The temperature and the duration of the soft-bake determine the residual concentration of solvent in the SU-8 at the moment of UV exposure and the onset of cross-linking. Higher T_{SB} and longer t_{SB} result in a lower solvent content. The observed behavior of the film thickness could be explained by higher shrinkage due to enhanced solvent evaporation at higher T_{SB} or longer t_{evap}. On the other hand, the solvent loss during soft-bake for films with comparable thickness is below 5% [26]. Therefore, the considerable decrease of thickness at $T_{SB} > 40$ °C has to be a result of partial development due to insufficient cross-linking of the photoresist. It has been shown by other authors that the residual solvent content during polymerization plays a major role in the processing of the SU-8 [27]. Low solvent content reduces the diffusion of the photo-acid and limits the mobility of the monomers in the polymer matrix. This reduces the cross-linking density of the SU-8 particularly if the PEB is done at low temperatures. In the case of thin SU-8 films, the high volatility of the solvent leads to a very fast decrease of the solvent content even at ambient temperature [28]. It is expected that there is a solvent gradient in the SU-8 because solvent evaporation takes place at the interface SU-8–air. Due to the reduced solvent content, the cross-linking density at the top of the SU-8 film is lower and non-cross-linked monomers are removed during the development step.

Higher residual solvent content seems to result in lower film stress. This behavior might be explained by a combination of several effects. The higher mobility of the SU-8 monomers at higher solvent content probably allows improved relaxation of the intrinsic stress during polymerization. The stress measurements presented in figures 1(*a*) and (*b*) seem to be correlated to the thickness of the SU-8. Thinner films show a considerable increase in film stress. This indicates that partial development of the SU-8 contributes to tensile stress. Therefore, the film stress could be directly related to the development step in PGMEA.

Figure 2 shows SEM micrographs of SU-8 chess-board patterns with a nominal base length of 10 μm. The experiments were performed in the second part of the soft-bake optimization and the only variable was the evaporation time t_{evap}. For $t_{evap} = 5$ min, loss of resolution and bad definition of the sidewalls were observed due to broadening of the SU-8 structures. On the other hand, $t_{evap} = 4$ h results in partial development of the square pattern. These experiments demonstrate the influence of the residual solvent content on the lithographic resolution. A higher amount of solvent due to shorter t_{evap} enhances diffusion of the photo-acid into non-exposed areas during the PEB and therefore leads to blurring of the original mask pattern. Lower solvent content hinders complete cross-linking of the exposed photoresist and leads to partial development at the edges, which is similar to the observations on the film thickness. Further, a nano-porous surface was observed for the sample processed at the highest solvent content (figure 2(*a*)). There, the solvent enclosed in the polymer evaporates after completed processing and leaves nano-pores in the resist. This is not observed for the resist processed with longer t_{evap} (figures 2(*b*) and (*c*)).

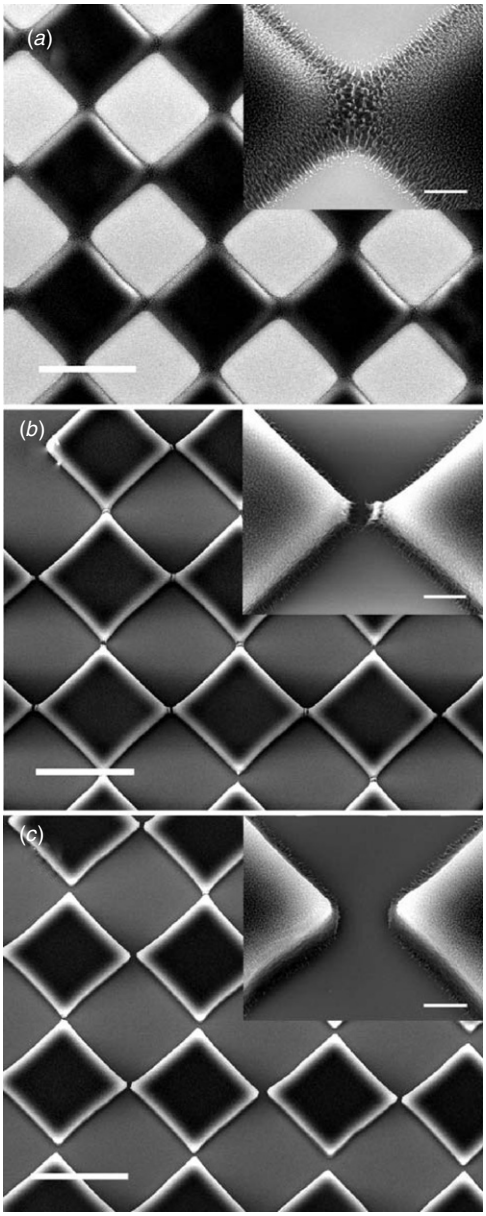

Figure 2. Resolution patterns for different t_{evap}. The nominal side length of the squares is 10 μm; (*a*) $t_{evap} = 5$ min: the SU-8 pattern (dark gray) is blurred due to acid diffusion into non-exposed areas; (*b*) $t_{evap} = 30$ min: good resolution; (*c*) $t_{evap} = 4$ h: insufficient cross-linking results in partial development of the SU-8. Scale bars: 10 μm in the main image and 1 μm in the inset.

A practical issue is stiction between the mask and photoresist if the exposure is done in hard contact mode. For 2 μm thick SU-8 films $t_{evap} < 15$ min resulted repeatedly in stiction of the substrate to the mask after exposure due to the higher solvent content in the resist. As a result of the observations on cross-linking, film stress, resolution and mask stiction, $t_{evap} = 30$ min was introduced between spin coating and exposure for further process optimization.

4. Influence of exposure and post-exposure bake

Figure 3(*a*) represents the result of the thickness measurements for samples processed at two different exposure doses with the

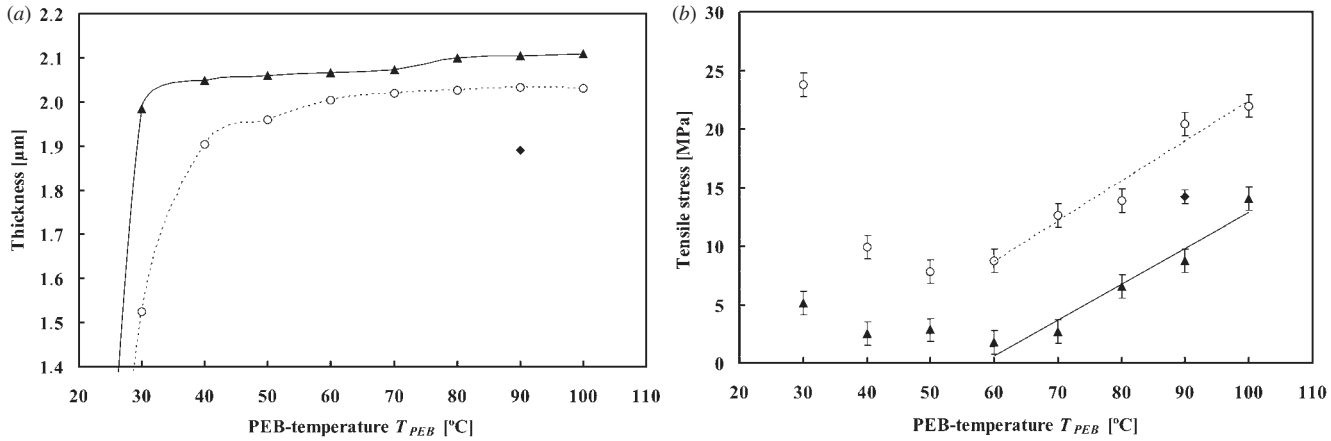

Figure 3. Influence of T_{PEB} on the (*a*) thickness and (*b*) tensile stress; (○) $D = 200$ mJ cm^{-2}; (▲) $D = 500$ mJ cm^{-2}; $t_{\mathrm{PEB}} = 60$ min; for comparison, the value for *Process A* is shown (♦).

extended range for T_{PEB}. A temperature as low as $T_{\mathrm{PEB}} = 50$ °C was sufficient to cross-link the SU-8 with the modified process sequence.

T_{PEB} was identified as the most important process parameter influencing the residual stress in thin SU-8 films. Figure 3(*b*) summarizes the measurements of the tensile film stress. Two temperature domains can be identified in figure 3.

- $T_{\mathrm{PEB}} < 50$ °C: the thickness of the SU-8 considerably decreases with a decrease in temperature and in parallel the stress increases.
- $T_{\mathrm{PEB}} \geqslant 60$ °C: the thickness of the SU-8 is more or less constant and the tensile film stress increases linearly with temperature.

Between the two temperature domains there is a process window where a minimum of tensile film stress is observed. The behavior of the film stress is similar for samples processed at different exposure doses. However, the absolute stress values are considerably lower at $D = 500$ mJ cm^{-2} compared to the ones at $D = 200$ mJ cm^{-2}. Further, the film thickness is higher for higher D. The duration of the PEB has only minor influence on the film thickness and stress. Longer t_{PEB} results in a slight decrease of the tensile stress and a higher thickness of the SU-8.

For $T_{\mathrm{PEB}} < 50$ °C, thermal stress is expected to be low according to (1). Nevertheless, the film stress is high in this temperature domain. Similar to the observations made during the soft-bake optimization presented above, this can be correlated to a reduced film thickness. The thermal energy seems to be too low to achieve sufficient cross-linking of the SU-8, and partial development results in high intrinsic stress. The thickness measurements in figure 3(*a*) show that there is less partial development of the SU-8 for $T_{\mathrm{PEB}} < 50$ °C if the exposure dose is increased to 500 mJ cm^{-2}. Higher D corresponds to a higher photo-acid concentration and therefore the cross-linking under identical bake conditions is improved.

For $T_{\mathrm{PEB}} \geqslant 60$ °C, intrinsic stress due to partial development is reduced and thermal stress is assumed to be dominant. The linear behavior of the tensile stress in figure 3(*b*) in this temperature domain follows the one predicted by (1) for a solidified polymer film on a silicon substrate subjected to thermal processing. This equation can be used to estimate the coefficient of thermal expansion (CTE) α_{SU8} of the SU-8:

$$\alpha_{\mathrm{SU8}} = \alpha_{\mathrm{Si}} + \beta \frac{1 - \upsilon_{\mathrm{SU8}}}{E_{\mathrm{SU8}}}. \tag{2}$$

Here, β is the slope of the linear approximation for $T_{\mathrm{PEB}} \geqslant 60$ °C as shown in figure 3(*b*). Young's modulus $E_{\mathrm{SU8}} = 3$ GPa [29] and Poisson's ratio $\upsilon_{\mathrm{SU8}} = 0.26$ [30] are assumed to be constant for the cross-linked polymer film. The CTE of silicon is $\alpha_{\mathrm{Si}} = 2.6 \times 10^{-6}$ K^{-1}. With (2) it is $\alpha_{\mathrm{SU8}} = 88.5 \times 10^{-6}$ K^{-1} for $D = 200$ mJ cm^{-2} and $\alpha_{\mathrm{SU8}} = 79.2 \times 10^{-6}$ K^{-1} for $D = 500$ mJ cm^{-2}. The calculated CTEs are in a first approximation independent of D and in the same order of magnitude as the values reported in the literature [31, 32].

For the samples processed at $T_{\mathrm{PEB}} \geqslant 60$ °C, the explanation of the offset in the stress values measured for different exposure doses is not very intuitive and is probably related to a difference in polymerization kinetics during the PEB. In the idealized case, a non-cross-linked SU-8 film is deposited on a silicon substrate and completely polymerized at the actual T_{PEB}. There, (1) can be used to estimate the increase of thermal stress during the cool-down to ambient temperature T_o. In reality, the experiments have shown that polymerization already is initiated at relatively low temperature during the ramping from T_o to T_{PEB} after UV exposure. There, thermal expansion of the pre-polymerized SU-8 results in a compressive stress component that has to be deduced from the value predicted by (1). It is expected that this kind of stress-hysteresis is more pronounced the more the film is pre-polymerized during temperature ramping. For higher D, polymerization is enhanced due to the availability of more photo-acid which therefore results in lower tensile film stress. Additional experiments showed that faster ramping leads to a considerable increase in residual stress as the time for partial polymerization is reduced. These observations demonstrate that exposure dose and temperature slopes during PEB are important process

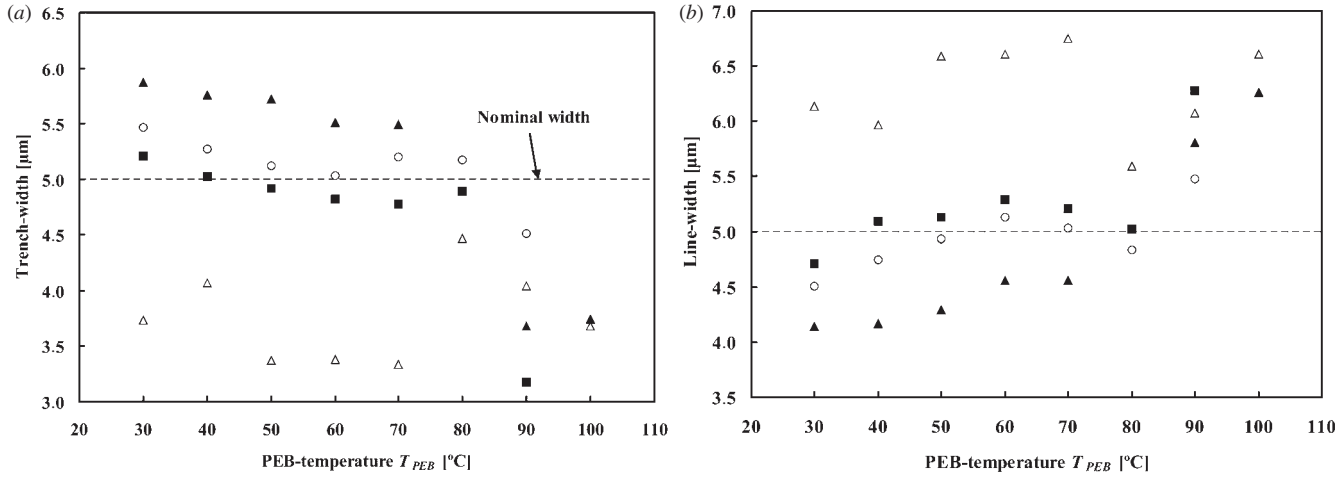

Figure 4. Influence of T_{PEB} on the dimension of (*a*) trenches and (*b*) lines with nominal width 5 μm; exposure dose *D*: (▲) 150 mJ cm^{-2}; (○) 200 mJ cm^{-2}; (■) 250 mJ cm^{-2}; (△) 500 mJ cm^{-2}.

parameters influencing the stress during processing of thin SU-8 films.

For comparison, the values of thickness and tensile stress for samples fabricated with *Process A* are also represented in figure 3. The measured values are identical for exposure doses of 250–500 mJ cm^{-2}. The value of tensile stress is about 14 MPa, which is assumed to be thermal stress due to the PEB at 90 °C. The thickness of the SU-8 is lower compared to the samples processed without soft-bake. This is explained by the volume loss due to evaporation of most of the solvent during soft-bake at $T_{SB} = 90$ °C performed in *Process A*.

The experimental investigation identified the exposure dose *D* as the most important parameter influencing the lithographic resolution. T_{PEB} also should be considered to obtain the desired resolution whereas t_{PEB} was less significant in the investigated range. Figure 4 shows measurements of the dimensions of trenches and lines with a nominal width of 5 μm to demonstrate the influence of *D* and T_{PEB} on the lithographic resolution.

At an increase of *D* and T_{PEB} a loss of resolution was observed. For the low exposure doses of 150–250 mJ cm^{-2} the behavior is similar. Figure 5 shows patterns obtained at $D =$ 200 mJ cm^{-2}. $T_{PEB} < 50$ °C results in partial development due to insufficient cross-linking. For $T_{PEB} > 70$ °C, line broadening and a decreased trench width are observed. The higher *D* the lower is T_{PEB} where nominal trench or line width is reached. The high dose of $D = 500$ mJ cm^{-2} results in overexposure independent of T_{PEB}. Higher t_{PEB} leads to a slight decrease of the resolution.

The important influence of the exposure dose on the resolution follows the expectations as it is the key parameter for all photolithographic processes. High *D* leads to line broadening and a reduced trench width due to optical effects such as diffraction at the mask and reflection on the substrate [15]. For the high value of $D = 500$ mJ cm^{-2}, these optical effects are dominant. The experiments at lower *D* demonstrate that besides the optical effects, photo-acid diffusion into non-exposed areas is an issue for processing of chemically amplified photoresists such as the SU-8. At high T_{PEB} the mobility of the photo-acid is increased and leads to a loss of resolution (figure 5(*c*)). Longer t_{PEB} allows for continued photo-acid diffusion although the effect is not as important as for the temperature.

The experiments allow the definition of an optimized *Process B* for the patterning of 2 μm thick SU-8 films. A solvent evaporation time $t_{evap} = 30$ min and a PEB of 60 min at a low $T_{PEB} = 50$–60 °C seem to be suitable to achieve polymerization of the SU-8, minimize residual stress and prevent loss of resolution. The exposure dose *D* should be high to improve cross-linking and reduce film stress. On the other hand, high exposure dose has a negative influence on the lithographic resolution. A value of $D = 250$ mJ cm^{-2} easily results in a trench resolution of 2 μm. This is the same resolution as the one achieved by the conventional *Process A*. For samples where the lithographic resolution is less critical, a higher exposure dose of 500 mJ cm^{-2} would further reduce thermal stress.

5. Fourier-transform infrared spectroscopy

Fourier-transform infrared (FT-IR) spectroscopy is a common method for the characterization of organic materials. Several authors have earlier reported FT-IR measurements to demonstrate the influence of the process parameters on the conversion of the epoxy groups of the SU-8 [15, 33, 34]. Here, the method was used to investigate the cross-linking achieved with *Process A* and *Process B*. The measurements were done in transmission mode and due to the limited sensitivity of the instrument (Perkin Elmer, Germany), the film thickness had to be increased to 5 μm compared to the other experiments. SU-8 2005 (MicroChem, USA) was spin-coated at 2000 rpm for 30 s with an acceleration of 5000 rpm s^{-1}. Due to the higher film thickness, the solvent evaporation time was increased to 2 h in *Process B*. For both processes, samples flood-exposed with 250 mJ cm^{-2} and with 500 mJ cm^{-2} were characterized with FT-IR. Completely non-cross-linked SU-8

Table 1. Relevant peaks of the SU-8 FT-IR spectra.

Wavenumber (cm^{-1})	Characteristic vibration	SU-8 processing effect on the peak intensity
861	C–O stretching of *cis* substituted epoxy rings	↘ with cross-linking
910	C–O stretching of *trans* substituted epoxy ring	↘ with cross-linking
1000–1230	C–O–C stretching in ethers	↗ with cross-linking
1000–1290	C–O stretching in phenols and secondary alcohols	↗ with cross-linking
1500	Aromatic C–C stretching (in-ring)	→ with cross-linking
1700–1750	C=O stretching cyclopentanone (solvent)	↘ with solvent evaporation

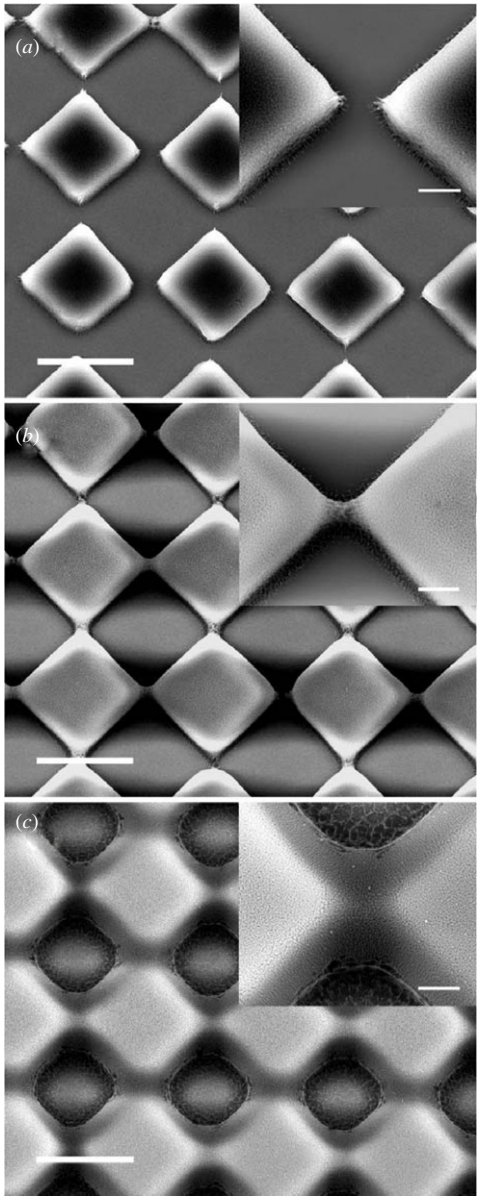

Figure 5. Resolution patterns for different T_{PEB}; $D = 200$ mJ cm^{-2}, $t_{PEB} = 60$ min; nominal side length of the squares is 5 μm; (*a*) $T_{PEB} = 30$ °C: insufficient cross-linking results in partial development of the SU-8; (*b*) $T_{PEB} = 70$ °C: good resolution; (*c*) $T_{PEB} = 90$ °C: the pattern is blurred due to photo-acid diffusion into non-exposed areas. Scale bars: 5 μm in the main image and 1 μm in the inset.

was used as a reference for the FT-IR measurements. For this purpose, an SU-8 monomer solution without the photo-initiator (Microresist, Germany) was spin-coated to a thickness of 5 μm and soft-baked for 60 min at 100 °C to remove the solvent.

Figure 6 represents a part of the recorded FT-IR spectra of the SU-8. The relevant peaks for the spectral analysis are summarized in table 1.

The spectra have been normalized to the absorption peak of the aromatic C–C stretching of the SU-8 monomer that is situated at 1500 cm^{-1}. This peak is independent of processing parameters as the monomer backbone is not modified during cross-linking [33]. During the polymerization of the SU-8, the epoxy groups of the monomers are opened and ether bonds and OH groups are formed instead. The peaks at 861 cm^{-1} and 910 cm^{-1} are assigned to C–O stretching of respectively *cis*- and *trans*-epoxy groups [35]. Both peaks are visible for the non-cross-linked monomer sample (figure 6(*a*)) and show reduced amplitude for the polymerized SU-8 (figures 6(*b*)–(*e*)). The lower amplitude of the absorption peaks for *Process B* compared to *Process A* shows that the new approach results in higher conversion of the epoxy groups. In parallel, the intensity of the C–O stretching band characteristic of ethers and secondary alcohols (respectively 1000–1230 cm^{-1} and 1000–1290 cm^{-1}) increases for the SU-8 samples processed by *Process B* (figures 6(*d*)–(*e*)), which is another consequence of the improved efficiency of cross-linking. For both processes, the amplitude of the epoxy peaks slightly decreases for $D = 500$ mJ cm^{-2} compared to $D = 200$ mJ cm^{-2}.

The FT-IR measurements confirm the influence of the solvent content on the processing of the SU-8. Higher solvent content due to the replacement of the soft-bake step with a solvent evaporation at ambient temperature allows higher mobility of photo-acid and SU-8 monomers. The result is a higher conversion of the epoxy groups in the thin SU-8 films. The FT-IR spectra demonstrate that this is the case although the PEB in *Process B* is done at a lower temperature $T_{PEB} = 50$ °C compared to $T_{PEB} = 90$ °C in *Process A*. For both processes, the FT-IR measurements indicate that the cross-linking density increases at higher exposure dose.

Figure 7 shows optical images of SU-8 patterns obtained by the same processes as the FT-IR samples. A mask in hard contact mode and $D = 250$ mJ cm^{-2} were used for the exposure. The structures fabricated with *Process A* show cracking at the concave corners due to film stress and insufficient structural stability. The absence of cracking for the film patterned with *Process B* is a direct visualization of the improved cross-linking combined with reduced thermal stress.

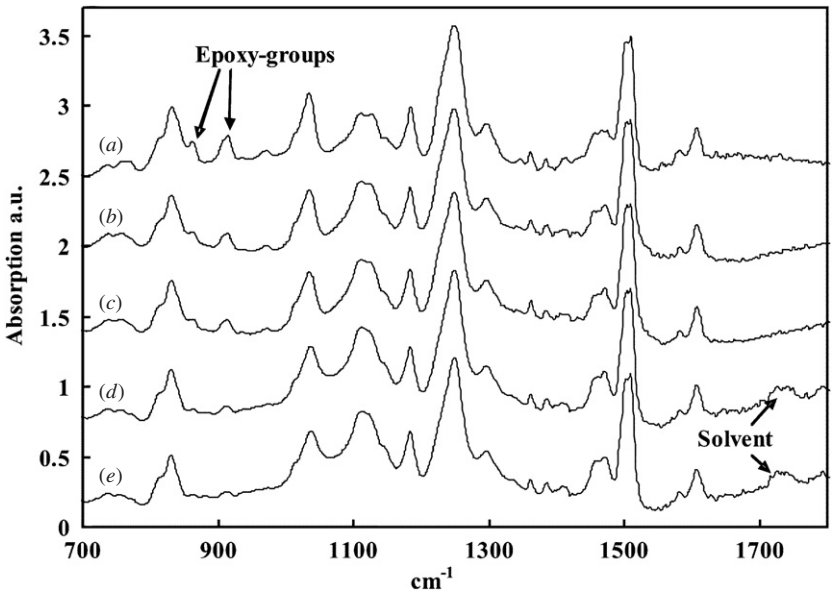

Figure 6. FT-IR spectra of 5 μm thick SU-8 films: (*a*) SU-8 monomer; (*b*) *Process A*, $D = 250$ mJ cm^{-2}; (*c*) *Process A*, $D = 500$ mJ cm^{-2}; (*d*) *Process B*, $D = 250$ mJ cm^{-2}; (*e*) *Process B*, $D = 500$ mJ cm^{-2}.

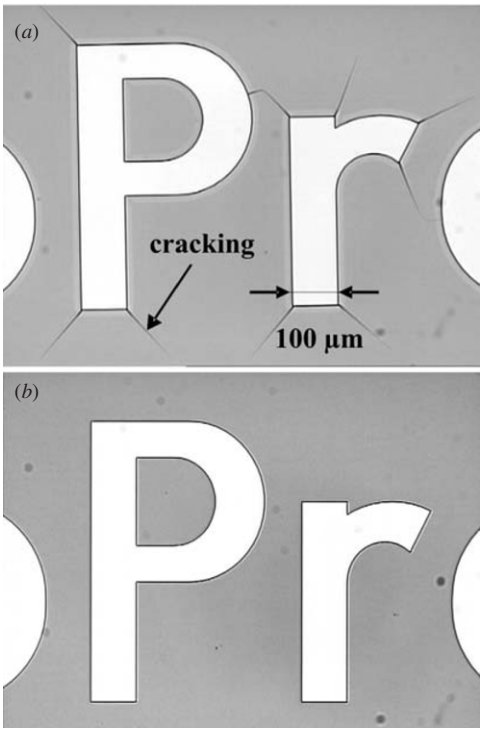

Figure 7. Optical images of 5 μm thick SU-8: (*a*) *Process A*; (*b*) *Process B*.

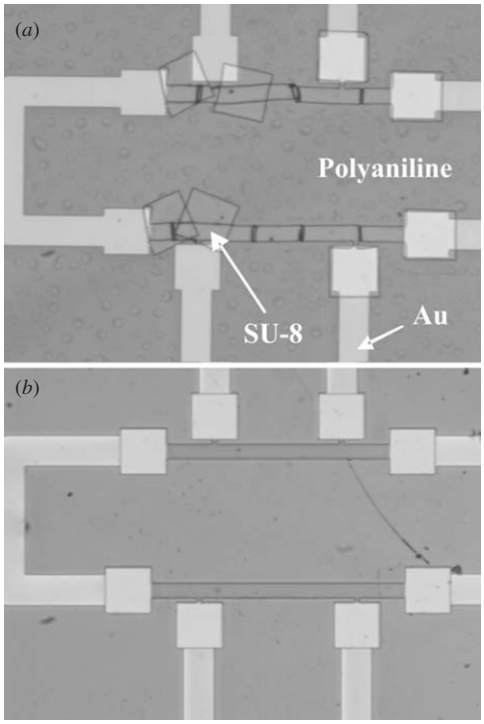

Figure 8. SU-8 patterned on top of a polyaniline film; (*a*) *Process A* results in delamination; (*b*) *Process B* leads to the perfect overlap of the SU-8 with the Au-electrode pads.

Furthermore, an absorption band around 1750 cm^{-1} is present only in the FT-IR spectrum of SU-8 films processed with *Process B* (figures 6(*d*)–(*e*)). This can be assigned to the SU-8 solvent cyclopentanone that shows an absorption band in this spectral region [36]. For the samples processed with a soft-bake step this band is absent (figures 6(*b*)–(*c*)). This observation indicates that the removal of the soft-bake results in higher residual solvent content in the cross-linked SU-8 films.

6. Optimized process design

Table 2 summarizes the influence of different process parameters on the investigated responses for thin SU-8 films with thicknesses in the micrometer range. This overview allows the adjustment of the parameters depending on the film thickness and on the requirements for the specific application. The residual stress is minimal for $T_{\mathrm{PEB}} = 50$ °C. The selection

Table 2. Summary of the influence of processing parameters on the investigated responses.

	Response (if corresponding parameter is increased)			
Parameter	Thickness	Residual stress[b]	Cross-linking	Resolution[c]
Solvent content[a]	↗	↘	↗	↘
Exposure dose D	↗	↘	↗	↘
PEB-time t_{PEB}	↗	↘	↗	↘
$T_{PEB} < 50$ °C	↗	↘	↗	↘
$T_{PEB} > 50$ °C	↗	↗	↗	↘

[a] The solvent content is regulated by the evaporation time t_{evap} or the soft-bake parameters.
[b] The residual stress is tensile.
[c] A decrease corresponds to a loss of resolution.

of a set of parameters aiming for increased cross-linking unfortunately results in a lower resolution. There, a trade-off has to be made.

The use of table 2 for the design of optimized processes is demonstrated with the example of a 2 μm thick SU-8 film used as an etch mask for the patterning of polyaniline by oxygen plasma. First, gold electrodes were patterned on a silicon substrate by a standard lift-off process. A polyaniline film with a thickness of 300 nm was deposited by spin coating and baked on a hotplate. On top of the unstructured polymer, a 2 μm thick SU-8 film was patterned. The critical issue for this application is the low adhesion between the SU-8 and the polyaniline. For *Process A*, tensile stress in the SU-8 film resulted in delamination of the structures as shown in figure 8(*a*). For this application, the optimized process design aimed for reduced film stress and high degree of cross-linking. The resolution was not a critical issue and therefore *Process B* with a high exposure dose of 625 mJ cm^{-2} was used. Figure 8(*b*) shows that the issue of delamination was solved with the optimized processing approach.

7. Conclusion

The residual solvent content is rarely discussed in the literature but it has an important influence on the cross-linking of thin SU-8 films. Higher solvent content facilitates the cross-linking reaction of the SU-8. This is a result of enhanced acid diffusion and higher mobility of the SU-8 monomers. Conventionally, a soft-bake is done in SU-8 processing. For thin SU-8 films, evaporation of the solvent is fast. Therefore, the soft-bake step was replaced by a short evaporation time at ambient temperature between spin coating and exposure of the photoresist. This resulted in lower tensile film stress and less partial development of the SU-8. On the other hand, higher solvent content leads to deterioration of the lithographic resolution, nano-porosity and to stiction of the substrate to the mask upon exposure. The duration of the solvent evaporation has to be adjusted depending on the film thickness. For a 2 μm thick SU-8 film, an evaporation time of 30 min is introduced, as a compromise between film stress and resolution.

The optimization of exposure and post-exposure bake showed that T_{PEB} is the main parameter influencing the stress and the cross-linking of thin SU-8 films. The increased solvent content due to the removal of the soft-bake allows polymerization of the SU-8 at a temperature as low as $T_{PEB} = 50$ °C. For $T_{PEB} < 50$ °C, high intrinsic film stress is generated due partial development as a result of insufficient cross-linking. For $T_{PEB} \geqslant 60$ °C, the difference in the coefficient of thermal expansion between the substrate and SU-8 results in higher tensile stress for samples processed at higher T_{PEB}. Higher T_{PEB} has a negative impact on the lithographic resolution due to enhanced diffusion of photo-acid into non-exposed areas. Processing at $T_{PEB} = 50$–60 °C seems to be suitable to minimize residual film stress and to prevent loss of resolution.

The exposure dose D should be high to improve cross-linking and reduce film stress. On the other hand, high exposure dose has a negative influence on the lithographic resolution. A value of $D = 250$ mJ cm^{-2} easily results in a trench resolution of 2 μm for 2 μm thick SU-8 films.

The results of the experimental investigation of the processing of thin SU-8 films allow the prediction of the influence of the processing parameters on process responses such as residual stress, structural stability, cross-linking density and lithographic resolution. With the gained knowledge on SU-8 processing an optimal resist process can be designed depending on the specific application. Although the conclusions are based on the processing of thin films ($t < 5$ μm), the observations might even be used for the process design for thicker SU-8 films. There, the solvent content probably has to be regulated by a short soft-bake at low temperature [14].

Acknowledgment

Funding was provided by the Danish Research Council for Technology and Production (FTP), project 2116-04-001.

References

[1] Gelorme J D, Cox R J and Gutierrez S A R 1989 *US Patent* 4882245
[2] LaBianca N, Gelorme J D, Lee K Y, Cooper E, O'Sullivan E and Shaw J 1993 *Electrochem. Soc. Proc.* **95-18** 386
[3] Lorenz H, Despont M, Fahrni N, LaBianca N, Renaud P and Vettiger P 1997 *J. Micromech. Microeng.* **7** 121

[4] Despont M, Lorenz H, Fahrni N, Brugger J, Renaud P and Vettiger P 1997 *MEMS '97, Proc., IEEE., 10th Ann. Int. Workshop Micro Electro Mech Syst., 1997* ed H Lorenz p 518
[5] Guerin L J, Bossel M, Demierre M, Calmes S and Renaud P 1997 *TRANSDUCERS '97 Chicago, 1997 Int. Conf. Solid State Sens. Actuators, 1997* ed M Bossel p 1419
[6] Jackman R J, Floyd T M, Ghodssi R, Schmidt M A and Jensen K F 2001 *J. Micromech. Microeng.* **11** 263
[7] Mogensen K B, El-Ali J, Wolff A and Kutter J P 2003 *Appl. Opt.* **42** 4072
[8] Balslev S, Jorgensen A M, Bilenberg B, Mogensen K B, Snakenborg D, Geschke O, Kutter J P and Kristensen A 2006 *Lab on a Chip* **6** 213
[9] Williams J D and Wang W 2004 *J. Microlithogr. Microfabrication Microsyst.* **3** 563
[10] Crivello J V 1999 *J. Polym. Sci.* A **37** 4241
[11] Glezos N, Patsis G P, Raptis I, Argitis P, Gentili M and Grella L 1996 *The 40th Int. Conf. Electron, Ion, and Photon Beam Technol. Nanofabrication (AVS, Atlanta, GA, USA)* p 4252
[12] Fedynyshyn T H, Szmanda C R, Blacksmith R F, Houck W E and Root J C 1993 *Proc. 16th Int. Symp. Electron, Ion, and Photon Beams (AVS, San Diego, CA, USA)* p 2798
[13] Patsis G P and Glezos N 2002 *J. Vac. Sci. Technol.* B **20** 1303
[14] Anhoj T A, Jorgensen A M, Zauner D A and Hubner J 2006 *J. Micromech. Microeng.* **16** 1819
[15] Zhang J, Chan-Park M B and Conner S R 2004 *Lab on a Chip* **4** 646
[16] Ling Z G, Lian K and Jian L 2000 *Advances in Resist Technology and Processing XVII* (Santa Clara, CA: SPIE) p 1019
[17] Schütz A 2004 *PhD Thesis* Technische Universität Berlin
[18] Bogdanov A L and Peredkov S S 2000 *Microelectron. Eng.* **53** 493
[19] Motahhari S and Cameron J 1999 *J. Reinf. Plast. Compos.* **18** 1011
[20] Gaynor J F and Desu S B 1994 *J. Mater. Sci. Lett.* **13** 236
[21] Genolet G, Brugger J, Despont M, Drechsler U, Vettiger P, de Rooij N F and Anselmetti D 1999 *Rev. Sci. Instrum.* **70** 2398
[22] Calleja M, Tamayo J, Johansson A, Rasmussen P, Lechuga L M and Boisen A 2003 *Sens. Lett.* **1** 20
[23] Friese C, Wissmann M and Zappe H 2003 *Sensors, 2003. Proc. IEEE* ed M Wissmann p 667
[24] www.microchem.com 2008
[25] Stoney G G 1909 *Proc. R. Soc* A **82** 172
[26] Shaw M, Nawrocki D, Hurditch R and Johnson D 2003 *Microsyst. Technol.* **10** 1
[27] Anhoj T A 2007 *PhD Thesis* Technical University of Denmark
[28] Uddin M, Chan H, Chow C and Chan Y 2004 *J. Electron. Mater.* **33** 224
[29] Hopcroft M, Kramer T, Kim G, Takashima K, Higo Y, Moore D and Brugger J 2005 *Fatigue Fract. Eng. Mater. Struct.* **28** 735
[30] Luo C, Schneider T W, White R C, Currie J and Paranjape M 2003 *J. Micromech. Microeng.* **13** 129
[31] Lorenz H, Laudon M and Renaud P 1998 *Microelectron. Eng.* **41–42** 371
[32] Feng R and Farris R J 2003 *J. Micromech. Microeng.* **13** 80
[33] Rath S K, Boey F Y C and Abadie M J M 2004 *Polym. Int.* **53** 857
[34] Tan T L, Wong D, Lee P, Rawat R S and Patran A 2004 *Appl. Spectrosc.* **58** 1288
[35] Parikh V M 1974 *Absorption Spectroscopy of Organic Molecules* (Menlo Park, CA: Addison-Wesley)
[36] www.sigma-aldrich.com 2008